length of the mRNA is equivalent to the length of pCDC (5). IKBKAP int-Ex20-int WT and IKBKAP int-Ex20-int FD were constructed in a similar way. Exon 20 (73 nt) with a flanking int sequence (127 nt upstream and 79 nt downstream) was amplified by PCR. The primers for plasmid construction are listed in Table S1.

Analysis of Transfected Cells. SH-SY5Y and HeLa cells were transfected with FuGeneHD according to the manufacturer's instructions. All plasmids used for transfection were prepared using a Midi prep kit (MACHEREY-NAGEL GmbH & Co.). Cells were grown in a monolayer in 12-well plates and then transfected with 0.5 μg per well of a reporter plasmid or cotransfected with 0.5 μg each of reporter plasmid and either plasmid expressing RNA binding protein. After a 24-h or 48-h incubation, cells were analyzed as follows. For semiquantitative RT-PCR analysis, cells were recovered with TRIzol (Invitrogen) (*SI Materials and Methods*, *Semiquantitative RT-PCR*). For microscopic analysis, cells were washed with PBS and then fixed with 4% (vol/vol) paraformaldehyde (Nacalai Tesque) for 10 min. The fixed cells were stained for 30 min with 5 μg/mL Hoechst 33342 (Sigma-Aldrich) and 1% Triton-X in PBS, and then washed with PBS once to remove excess Hoechst. After staining the nucleus, cells were kept in PBS and visualized using an Olympus IX81 microscope with a DP72 digital camera (Olympus).

Semiquantitative RT-PCR. Total RNAs were prepared from cultured cells with TRIzol according to the manufacturer's instructions. If necessary, the RNAs were treated with RNase-free DNase (RQ1; Promega) according to the manufacturer's manual. First-strand cDNA was synthesized using RT (Prime Star; Takara Bio, Inc.) with random hexamers and amplified by PCR using an appropriate set of primers. Semiquantitative RT-PCR was performed with Ex Taq polymerase (Takara Bio, Inc.). Cycle conditions were as follows: 94 °C for 2 min; followed by 28 cycles (reporter), 38 cycles (*IKBKAP*), or 23 cycles (*GAPDH*) of denaturation at 94 °C for 10 s; annealing at 50 °C (*IKBKAP*) or 58 °C (*GAPDH*) for 30 s; and elongation at 72 °C for 30 s, with a final incubation at 72 °C for 5 min in a PCR thermal cycler (BIOMETRA). PCR products were separated by electrophoresis and stained with ethidium bromide. Images were obtained with a gel imaging system (ChemiDoc; Bio-Rad Laboratories). The primers for semiquantitative RT-PCR are listed in Table S1.

Small Chemical Compounds. A total of 620 compounds from the Prestwick Chemical Library (Prestwick Chemicals), and 18 compounds (Namiki Shoji Co., Ltd.) provided by the Medical Research Support Center, Graduate School of Medicine, Kyoto University, were screened. Part of the library was newly synthesized by following the procedures described in *SI Materials and Methods* (*Synthesis of Small Chemicals*). Kinetin powder was purchased from Nacalai Tesque.

Fluorescence Quantification in Cell-Based Screening of Small Chemical Compounds. The visualized images of the expression of *IKBKAP-FD* reporter in HeLa cells were analyzed, and the GFP/RFP ratio was calculated using the compartment analysis algorithm (Thermo Fisher Scientific). Because E19/20/21-GFP proteins were predominantly in the nucleus, whereas E19/21-RFP proteins were mainly in the cytoplasm, we were able to take advantage of the compartment analysis algorithm. The compartment analysis algorithm was used to define the primary object, to apply a nucleic mask and a cytoplasmic mask, and to quantify GFP and RFP intensity in the masks, respectively. The primary object was defined as the nucleus by Hoechst staining. The nucleic mask was set as inside an area one pixel smaller than the primary object. The cytoplasmic mask was defined as the area one to five pixels outside of the primary object. The score was calculated as the mean of each value of the GFP/RFP ratio of an object.

In Vitro Splicing and Complex Formation Assay. The templates, CDC-IKBKAP Ex20WT and CDC-IKBKAP Ex20FD, were linearized with SmaI. In vitro transcription and purification of the transcribed RNAs were performed as described previously (5). In vitro splicing was also conducted as described previously (6), except that HeLa cell nuclear extracts (CIL BIOTECH) were preincubated with DMSO (0.05%) or RECTAS (20 μM) (at 37 °C for 15 min) and with pre-mRNA (at 37 °C for an additional 10 min) before the splicing reaction. The splicing reaction was incubated at 30 °C. RNA was analyzed by 6% (vol/vol) polyacrylamide denaturing PAGE. The gels were dried under vacuum and visualized by a phosphorimager. Spliceosomal complexes were analyzed by mixing 5 μg of heparin with a 12.5-μL splicing reaction at each time point and incubated at room temperature for 10 min. The complexes were analyzed in a loading buffer with a final concentration of 50 mM Tris·glycine, 4% (vol/vol) glycerol, 0.25% xylene cyanol, and bromophenol blue on a 2% (wt/vol) agarose (Seakem GTG agarose) gel run in 50 mM Tris·glycine at 50 V for 4 h at room temperature. The E-complex assay was performed as previously described (7), with 37 °C preincubation for 10 min. The E-complex was formed by a 30 °C incubation, and heparin (1.6 μg per lane) was added and incubated for a further 10 min where indicated.

Single-Dose Oral Administration. RECTAS or kinetin at a dose of 50 mg or 100 mg suspended in 0.5% carboxymethylcellulose was administered orally to male Jcl:ICR 7-wk-old mice (Charles River Laboratories). These mice were anesthetized at each time point with pentobarbital (Mylan), and blood was sampled, allowed to clot, and centrifuged for serum preparation. Mice were perfused with saline, and brains were removed. Brain homogenates were prepared using Polytron (Kinematica) in saline. Levels of RECTAS or kinetin in brain supernatants and serum were analyzed by LC/MS using an Agilent 6420 Q-TOF mass spectrometer with an Agilent 1290 nano-flow HPLC system (Agilent Technologies) and a ZORBAX HILIC Plus (Kinetin) or ZORBAX Eclipse Plus C18 (RECTAS) column (Agilent Technologies).

Immunoblot. Total proteins were extracted from the cells by scraping with CelLytic MT Cell Lysis Reagent (Sigma-Aldrich) containing a protease inhibitor mixture (Roche). After 10 min of centrifugation at 17,800 × *g* at 4 °C, the supernatant was collected and protein concentrations were measured using a Bio-Rad Protein Assay Kit (Bio-Rad). Proteins were separated via 5–20% gradient SDS/PAGE and then transferred onto a polyvinylidene fluoride membrane (Millipore) by electroblotting. The membranes were blocked with 5% (wt/vol) skim milk in PBS and probed with a mouse anti-IKAP antibody (Abcam) at 1:1,000 or a mouse anti-GAPDH antibody (Ambion) at 1:4,700 overnight at 4 °C, followed by incubation with HRP-conjugated secondary antibody [i.e., goat anti-mouse IgG HRP (Abcam)] at 1:5,000. Immunoblots were visualized by an ECL reaction with the ImmunoStar Kit (Wako Chemicals USA) or Chemi-Lumi One (Nacalai Tesque) and were detected with ChemiDoc.

Expression Analysis. We performed expression analysis with Affymetrix GeneChip Human Exon 1.0 ST arrays. Cells from FD patient no. 42 were plated on a six-well plate at 1×10^5 cells per well in 2 mL of complete medium. After 3 d of culture, cells were treated with 0.1% DMSO or 2 μM RECTAS in flesh medium at 37 °C and 5% CO_2 for an additional 6 h. After treatment, total RNA was extracted using TRIzol reagent, and the RNA quality was evaluated with an Agilent 2100 Bioanalyzer RNA NanoChip system (Agilent Biotechnologies). For the microarray experiment, biotin-labeled RNA was prepared using 100 μg of total RNA. The first cDNA, cRNA, and second cDNA were synthesized using an Ambion WT Expression Kit as described by the manufacturer (Ambion). The second cDNA was then fragmented using uracil

DNA glycosylase and apurinic/apyrimidic endonuclease-1, and biotin-labeled with terminal deoxynucleotidyl transferase using a GeneChip WT Terminal Labeling Kit (Affymetrix). Hybridization was performed using 5 μg of the biotinylated target, which was incubated with the GeneChip Human Exon 1.0 ST array at 45 °C for 16 h. After hybridization, nonspecifically bound material was removed by washing, and specifically bound target was detected using a GeneChip Hybridization, Wash and Stain Kit, and a GeneChip Fluidics Station 450 (both from Affymetrix). The arrays were scanned using a GeneChip Scanner 3000 7G (Affymetrix), and raw data were extracted from the scanned images and analyzed with the Affymetrix Power Tools software package. Expression values for each array probe were calculated by the RMA method using Affymetrix Expression console software. Bioinformatic analyses for detecting altered splicing events were performed as described previously (8). If an exon had >1.2- or <0.833-fold change in expression between the control and RECTAS treatments, and if the differences among the fold changes of the other exons in a gene were >2.5 SD, we defined it as altered exon splicing. In this analysis, we calculated relative expression values based on fold changes normalized with gene expression values to cancel out the effects of gene expression changes. We drew a heat map with these normalized expression values for exons for which alteration of splicing regulation had been defined. The heat map was drawn with the MultiExperiment Viewer (MeV) data analysis tool (9).

We also analyzed expression profiles of the genes with the dataset. We calculated the expression values of a gene as the mean of the expression values of the exons constituting the gene. We set the threshold for detecting up- or down-regulated genes under RECTAS treatments as fold changes that were >1.3 or <0.77, respectively, and P values of t tests as <0.01. These calculations were performed using Perl scripts and the R statistical package (www.r-project.org).

Sequence Analysis. We used the hg18 human genome for sequence analyses, according to exon array design. For construction of the control exon set, we listed 4,192 exons from genes that included RECTAS-responding exons, but did not respond to RECTAS per se, as an initial pool of control exons. We randomly chose 100 exons from this pool and used them as the control exon set.

The SpliceAid program was redeveloped with Perl for computing on a local environment. Information on the *cis*-element was obtained from the SpliceAid webpage. According to description on the webpage, *cis*-elements on exon regions and with positive scores were treated as ESEs and those *cis*-elements with negative scores were treated as ESSs. We used the statistical environment R to draw box plots. In the box plots, positions of the maximum and minimum values within the ranges from the first quarter + 1.5 * interquartile range (IQR) to the third quarter − 1.5 * IQR, whereas IQR was defined as the third − first quarters, are shown as horizontal lines outside of the boxes and joined to the boxes with vertical lines.

For the MEME study, we found motifs with lengths of 6, 8, and 10. With each parameter, we listed 50 motifs. We had three datasets (inclusion-type, exclusion-type, and control exon sets) from which we obtained 450 motif candidates. Existence of the motifs in the exon sequences was tested with the "mast" program in the MEME program set, with the parameter "–mt 1e-3."

RNA Preparation for tRNA Modification Analysis. For tRNA modification analysis in carrier cells and cells of patient nos. 42 and 50, total RNAs were recovered from cells cultured for 2 d after confluency (cultured for 7 d in total). The time course in carrier cells and cells of patient no. 42 with or without RECTAS treatment is described in the main text. Total RNAs were prepared from cultured cells with TRIzol and precipitated with 2-propanol according to the manufacturer's instructions. The RNA pellet was dried and stored. For RCC isolation of tRNA, the RNA pellets were dissolved in water and purified by anion exchange chromatography. Briefly, the RNA samples were applied to 1 mL of DEAE Sepharose FF (GE Healthcare) in 5-mL disposable columns (Bio-Rad) equilibrated with 5 mL of buffer A [10 mM Hepes-KOH (pH 7.5), 200 mM NaCl, and 2 mM DTT]. The RNA samples on DEAE Sepharose were washed with buffer A and then eluted with buffer B [10 mM Hepes-KOH (pH 7.5), 1 M NaCl, and 2 mM DTT].

Human $tRNA^{Val}$(UAC), $tRNA^{Arg}$(UCU), and $tRNA^{Gly}$(UCC) were homogeneously isolated by the RCC method using an RCC device, following the previously described method with a minor modification (10). The 5′-terminal amino-modified DNA probes were covalently immobilized on NHS-activated Sepharose 4 Fast Flow (GE Healthcare) according to the manufacturer's instructions. The DNA resins were packed into the special tips that were attached to multichannel head of the RCC device. DNA probes for RCC are listed in Table S1. A tRNA fraction enriched by DEAE chromatography (55–200 μg) that was dissolved in 2 mL of 6× NME buffer [1.2 M NaCl, 30 mM MES·NaOH (pH 6.0), 15 mM EDTA, and 1 mM DTT] was passed through and captured by affinity tip columns by pipetting the RNA mixture 40 times at 66 °C. Unbound RNAs were washed by pipetting in 700 μL of 0.1× NME buffer [20 mM NaCl, 0.5 mM MES·NaOH (pH 6.0), 0.25 mM EDTA, and 0.5 mM DTT] in series, followed by eight washes with 600 μL of 0.1× NME buffer at 40 °C. RNAs were eluted from the column with three washes of 400 μL or 600 μL of 0.1× NME buffer at 68 °C. The eluted RNAs were precipitated with ethanol. The total yield from each tip column was calculated by measuring UV absorbance at 260 nm.

LC/MS Analysis of tRNAs. One picomole of isolated tRNA was digested with 50 U RNase T_1 (Epicentre) in 20 mM NH_4OAc (pH 5.3) at 37 °C for 60 min. After digestion, an equal volume of 0.1 M triethylamine acetate (pH 7.0) was added to the reaction solution. The digest (0.5 pmol) was analyzed using a linear iontrap–orbitrap hybrid mass spectrometer (LTQ Orbitrap XL; Thermo Fisher Scientific) equipped with a custom-made nanospray ion source, a splitless nano-HPLC system (DiNa; KYA Technologies), a C18 trap cartridge (HiQ sil C18HS-3; KYA Technologies), and a C18 capillary column (KYA Technologies).

Northern Blotting. The total RNAs used for Northern blotting were the same as used in the tRNA modification analysis by RCC and LC/MS. Four micrograms of the total RNA was electrophoresed on a 10% (vol/vol) polyacrylamide gel containing 7 M urea and blotted onto a nylon membrane (Hybond N+; Amersham Biosciences) with 0.5× TBE. The membrane was air-dried, and the blotted RNA was fixed onto the membrane by UV irradiation (254 nm, 120 mJ/cm^2). Northern blotting was conducted using a standard protocol (11). Oligonucleotide probes were end-labeled with [γ-^{32}P]ATP. Radioactivity was visualized by exposing the membrane to an imaging plate and analyzing with a bioimaging analyzer (Typhoon; GE Healthcare). The sequences of oligonucleotide probes were identical for RCC isolation.

Cell Viability Assay. Cells were pretreated with DMSO or RECTAS before plating into a 96-well plate for ~4–5 d. The pretreated cells were seeded into 96-well plates at a density of 0.3×10^4 cells per well in complete medium, and ~2–3 h later, DMSO (0.02%) or RECTAS (10 μM) was added. Cell viability was measured at the indicated time points using the Cell Titer Glo Assay Kit according to manufacturer's instructions (Promega).

Synthesis of Small Chemicals.

General remarks. All reactions were performed in dried glassware in an atmosphere of argon, unless otherwise noted. The melting

point was measured on a YANACO MP-J3 instrument or an Opti Melt MPA100 (both from Stanford Research Systems) and is uncorrected. ^{1}H NMR spectra were obtained with a Bruker AVANCE 500 spectrometer at 500 MHz. ^{19}F NMR spectra were obtained with a Bruker AVANCE 400 spectrometer at 376 MHz. DMSO-d_6 (catalog no. DLM-10; CIL BIOTECH) was used as a solvent for obtaining NMR spectra. Chemical shifts (δ) are given in parts per million down-field from the solvent peak (δ 2.49 for ^{1}H NMR) as an internal reference or as α,α,α-trifluorotoluene (δ-63.0 ppm for ^{19}F NMR in $CDCl_3$) as an external standard with coupling constants given in hertz. High-resolution mass spectra were measured on a Bruker micrOTOF mass spectrometer under negative electrospray ionization conditions.

2-Furylmethylamine (catalog no. F0091) and 6-chloro-2-fluoropurine (catalog no. C2221) were purchased from Tokyo Chemical Industry Co., Ltd. 2,6-Dichloropurine (catalog co. 322-35482), acetonitrile (catalog no. 014-00386), and triethylamine (catalog no. 202-02646) were purchased from Wako Pure Chemical Industries, Ltd. All other chemical reagents used were of commercial grade and were used as received.

2-Chloro-6-(2-furylmethyl)purine (RECTAS).

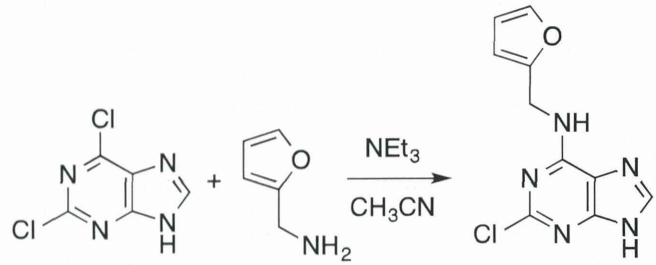

To a mixture of 2,6-dichloropurine (189 mg, 1.00 mmol) and 2-furylmethylamine (97.0 mg, 1.00 mmol) dissolved in acetonitrile (20 mL) was added triethylamine (0.150 mL, 1.08 mmol) at room temperature. After stirring for 3 h at 60 °C, the resulting precipitate was collected by filtration, washed with water and diethyl ether, and dried in vacuo to give 2-chloro-6-(2-furylmethyl)purine (19.8 mg, 0.0795 mmol, 8.0%) as a colorless solid. The spectra data of the product were identical to those spectral data reported in the literature (12).

1. Keith G (1984) The primary structures of two arginine tRNAs (anticodons C-C-U and mcm5a2U-C-psi) and of glutamine tRNA (anticodon C-U-G) from bovine liver. *Nucleic Acids Res* 12(5):2543–2547.
2. van den Born E, et al. (2011) ALKBH8-mediated formation of a novel diastereomeric pair of wobble nucleosides in mammalian tRNA. *Nat Commun* 2:172.
3. Chheda GB, Patrzyc HB, Tworek HA, Dutta SP (1999) Isolation and characterization of 5-carbamoylmethyluridine and 5-carbamoylmethyl-2-thiouridine from human urine. *Nucleosides Nucleotides* 18(10):2155–2173.
4. Keith G, et al. (1990) Eukaryotic tRNAs(Pro): Primary structure of the anticodon loop; Presence of 5-carbamoylmethyluridine or inosine as the first nucleoside of the anticodon. *Biochim Biophys Acta* 1049(3):255–260.
5. Kataoka N, et al. (2000) Pre-mRNA splicing imprints mRNA in the nucleus with a novel RNA-binding protein that persists in the cytoplasm. *Mol Cell* 6(3):673–682.
6. Rahman MA, et al. (2013) HnRNP L and hnRNP LL antagonistically modulate PTB-mediated splicing suppression of CHRNA1 pre-mRNA. *Sci Rep* 3:2931.
7. Ohe K, Mayeda A (2010) HMGA1a trapping of U1 snRNP at an authentic 5′ splice site induces aberrant exon skipping in sporadic Alzheimer's disease. *Mol Cell Biol* 30(9): 2220–2228.
8. Yamashita Y, et al. (2012) Four parameters increase the sensitivity and specificity of the exon array analysis and disclose 25 novel aberrantly spliced exons in myotonic dystrophy. *J Hum Genet* 57(6):368–374.
9. Saeed AI, et al. (2006) TM4 microarray software suite. *Methods Enzymol* 411:134–193.
10. Miyauchi K, Ohara T, Suzuki T (2007) Automated parallel isolation of multiple species of non-coding RNAs by the reciprocal circulating chromatography method. *Nucleic Acids Res* 35(4):e24.
11. Tomita K, Ogawa T, Uozumi T, Watanabe K, Masaki H (2000) A cytotoxic ribonuclease which specifically cleaves four isoaccepting arginine tRNAs at their anticodon loops. *Proc Natl Acad Sci USA* 97(15):8278–8283.
12. Novotná R, Trávníček Z, Popa I (2010) X-ray crystallographic and NMR study of the tautomerism in kinetin, kinetin riboside and their derivatives: A comparison between the solid state and solution. *J Mol Struct* 963(2-3):202–210.
13. McLuckey SA, Van Berkel GJ, Glish GL (1992) Tandem mass spectrometry of small, multiply charged oligonucleotides. *J Am Soc Mass Spectrom* 3(1):60–70.
14. Johansson MJ, Esberg A, Huang B, Björk GR, Byström AS (2008) Eukaryotic wobble uridine modifications promote a functionally redundant decoding system. *Mol Cell Biol* 28(10):3301–3312.

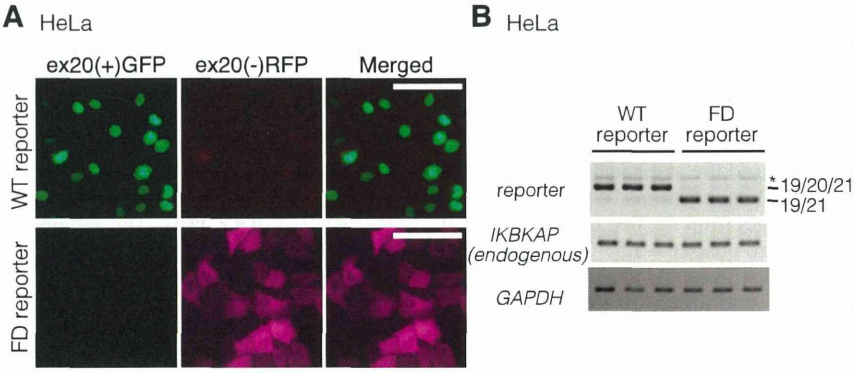

Fig. S1. Visualization of disease-specific splicing using the SPREADD system. (*A*) Microscopic analysis of HeLa cells expressing the *IKBKAP-WT* reporter (*Upper*) and the *IKBKAP-FD* reporter (*Lower*). The results are presented as in Fig. 1*C*. (Scale bar: 100 μm.) (*B*) RT-PCR analysis of mRNAs derived from HeLa cells expressing the *IKBKAP-WT* reporter or the *IKBKAP-FD* reporter. The results are presented as in Fig. 1*D*. An asterisk indicates the PCR product corresponding to a hybrid of 19/20/21 and 19/21.

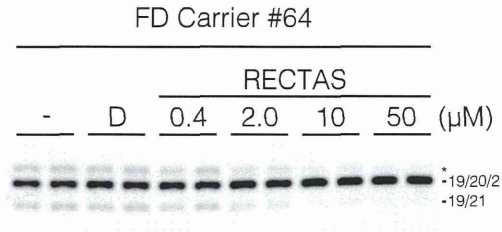

Fig. S2. Promotion of exon 20 inclusion with endogenous *IKBKAP* pre-mRNAs in carrier cells treated with RECTAS. RT-PCR analyses of endogenous *IKBKAP* mRNAs in carrier fibroblasts treated with the indicated concentrations of RECTAS were conducted. D, DMSO control; -, medium change only.

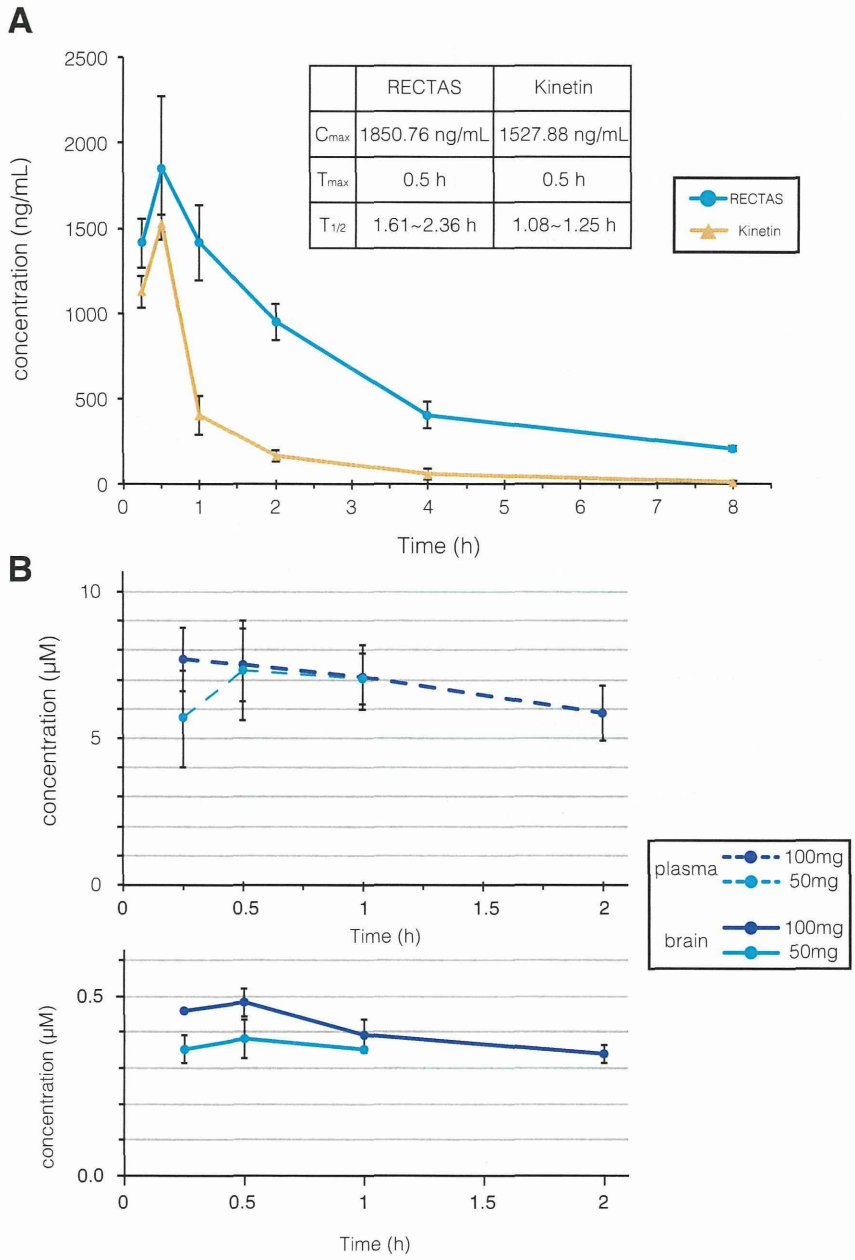

Fig. S3. Pharmacokinetic profile of RECTAS after oral administration to mice. (*A*) Mean concentration in plasma vs. time profile of RECTAS and kinetin in imprinting control region (ICR) mice after oral administration of a single 50-mg/kg dose of RECTAS or kinetin. Each time point is the mean ± SEM ($n = 3$). The first collection time was 15 min after the administration of compounds. (*B*) Mean concentration in the plasma (*Top*) and brain (*Bottom*) vs. time profile of RECTAS in ICR mice after oral administration of a single 50- or 100-mg/kg dose of RECTAS. Each time point is the mean ± SEM ($n = 3$). The first collection time was 15 min after the administration of compounds.

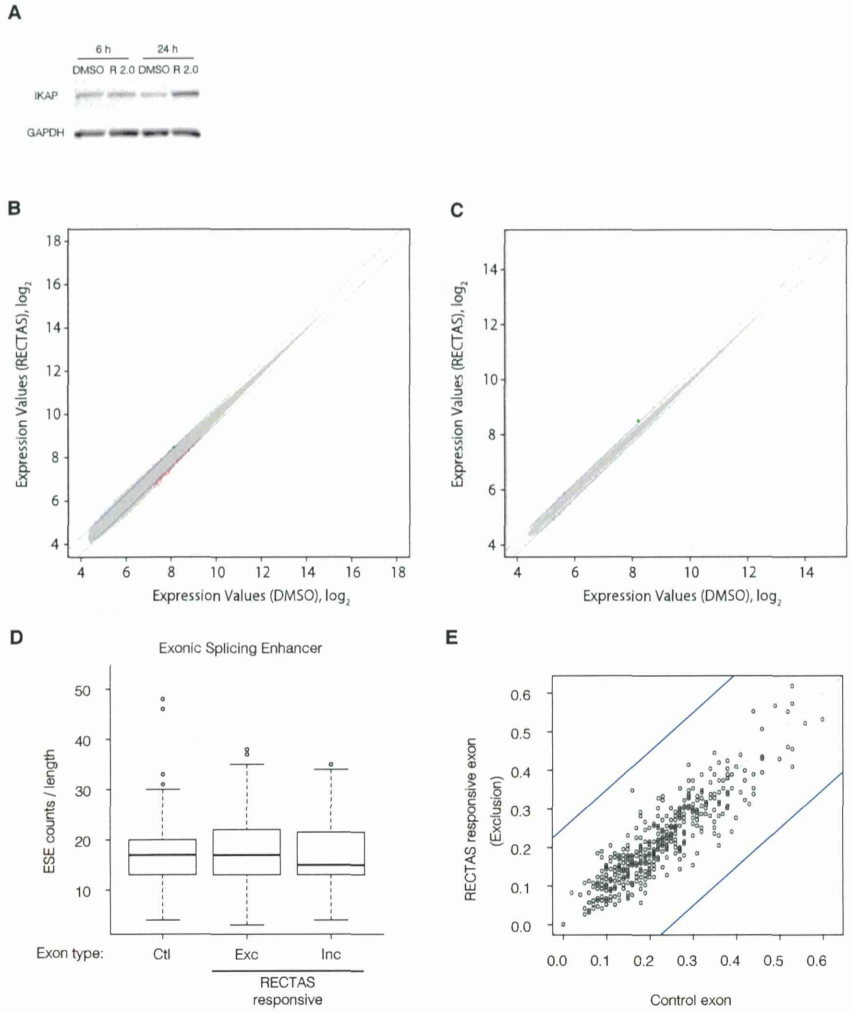

Fig. S4. Splicing events and gene expression influenced by treatment with RECTAS. (*A*, *Top*) IKAP expression in cells of FD patient no. 42 treated with DMSO or 2 μM RECTAS for 6 or 24 h. (*A*, *Bottom*) GAPDH was used as a control. (*B*) Scatter plots show the expression values (log_2) of each exon in the indicated pairs of treatment (RECTAS vs. DMSO). Spots with values that changed by more than the threshold are highlighted in red ($P < 0.01$). (*C*) Scatter plots show the expression values (log_2) of each gene in the indicated pairs of treatment (RECTAS vs. DMSO). Spots with values that changed greater than the threshold are highlighted in red ($P < 0.01$). The *IKBKAP* spot is highlighted in green. (*D*) Tukey box plots show count comparisons of ESE per 100 bases of exon sequences. The plots are as described in Fig. 4*B*. Ctl, control exons; Exc, exclusion-type exons; Inc, inclusion-type exons. (*E*) Comparisons of fractions of exons with sequence motifs between exclusion-type exons and control exons. The plots are as described in Fig. 4*C*.

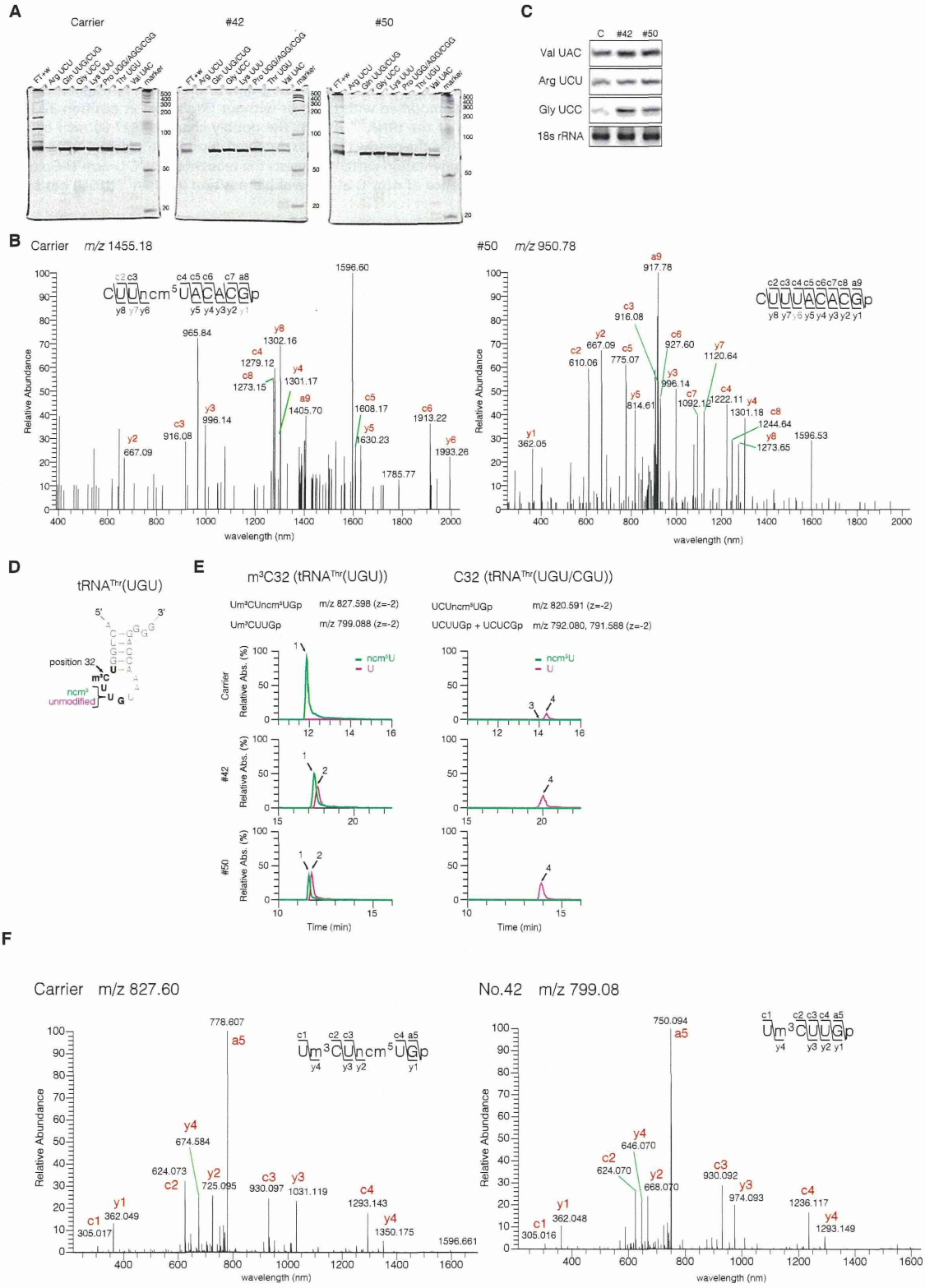

Fig. S5. Isolation of tRNAs by RCC and MS analysis of an anticodon-containing fragment in tRNA^{Val}(UAC). (*A*) PAGE (10%, 7 M urea) of tRNAs from cells derived from patients with FD or a carrier, isolated by RCC. RNAs were visualized by SYBR Gold staining. (*B*) CID spectrum of the anticodon fragment from RNase T_1 digests of the tRNA^{Val}(UAC). The doubly charged (1,455.18 *m/z*) or quadruply charged (950.78 *m/z*) ions were used as precursor ions for CID. The letters in gray indicate that the product ion was detected in other CID spectra using different charged ions as precursors. The nomenclature used for product ions is defined in the literature (13). The fragmentation pattern suggests the sequence C-U-U-ncm^{5}U-A-C-A-C-Gp or C-U-U-U-A-C-A-C-Gp as indicated in the carrier or FD patient #50, respectively. Because the presence of mcm^{5}s^{2}U and mchm^{5}U at the wobble position has been reported in bovine tRNA^{Arg}(UCU) and tRNA^{Gly}

Legend continued on following page

(UCC), respectively (1, 2), and it was suggested that tRNA^{Val}(UAC) contains ncm^{5}U at the wobble position (3, 4), we assumed that these human tRNAs also contained the modifications described above. (*C*) Northern blot analysis of tRNAs Val(UAC), Arg(UCU), and Gly(UCC) in carrier cells (C) and cells of FD patients #42 and #50; 18s rRNA was used as a loading control. (*D*) Secondary structure with the sequences at the anticodon stem–loop region of tRNA^{Thr}(UGU) is shown. The wobble uridine residue of the tRNA is indicated with possible modifications. The reported modifications m^{3}C near the anticodon are also indicated. The sequences indicated in bold letters are the RNase T_1 fragments harboring the anticodon. (*E*) Mass chromatograms of the RNase T_1 fragments of tRNA^{Thr}(UGU) are shown as in Fig. 5 *B–D*. The mass chromatograms of the RNase T_1 fragments modified with (*Left*) or without (*Right*) m^3 at position 32 (C32) are shown separately. (*F*) CID spectrum of the anticodon fragment from RNase T_1 digests of the tRNA^{Thr} (UGU). The doubly charged (827.60 *m/z*) or doubly charged (799.08 *m/z*) ions were used as precursor ions for CID. The letters in gray indicate that the product ion was detected in other CID spectra using different charged ions as precursors. The nomenclature used for product ions is as in Fig. S5*B*. The fragmentation pattern suggests the sequence C-m^{3}C-U-ncm^{5}U-Gp or U-m^{3}C-U-U-Gp as indicated in the carrier or in FD patient no. 42, respectively. Because the presence of ncm^{5}U at the wobble position in tRNA^{Thr}(UGU) has been reported in yeast (14), we assume that the wobble uridine is also modified with ncm^{5}U.

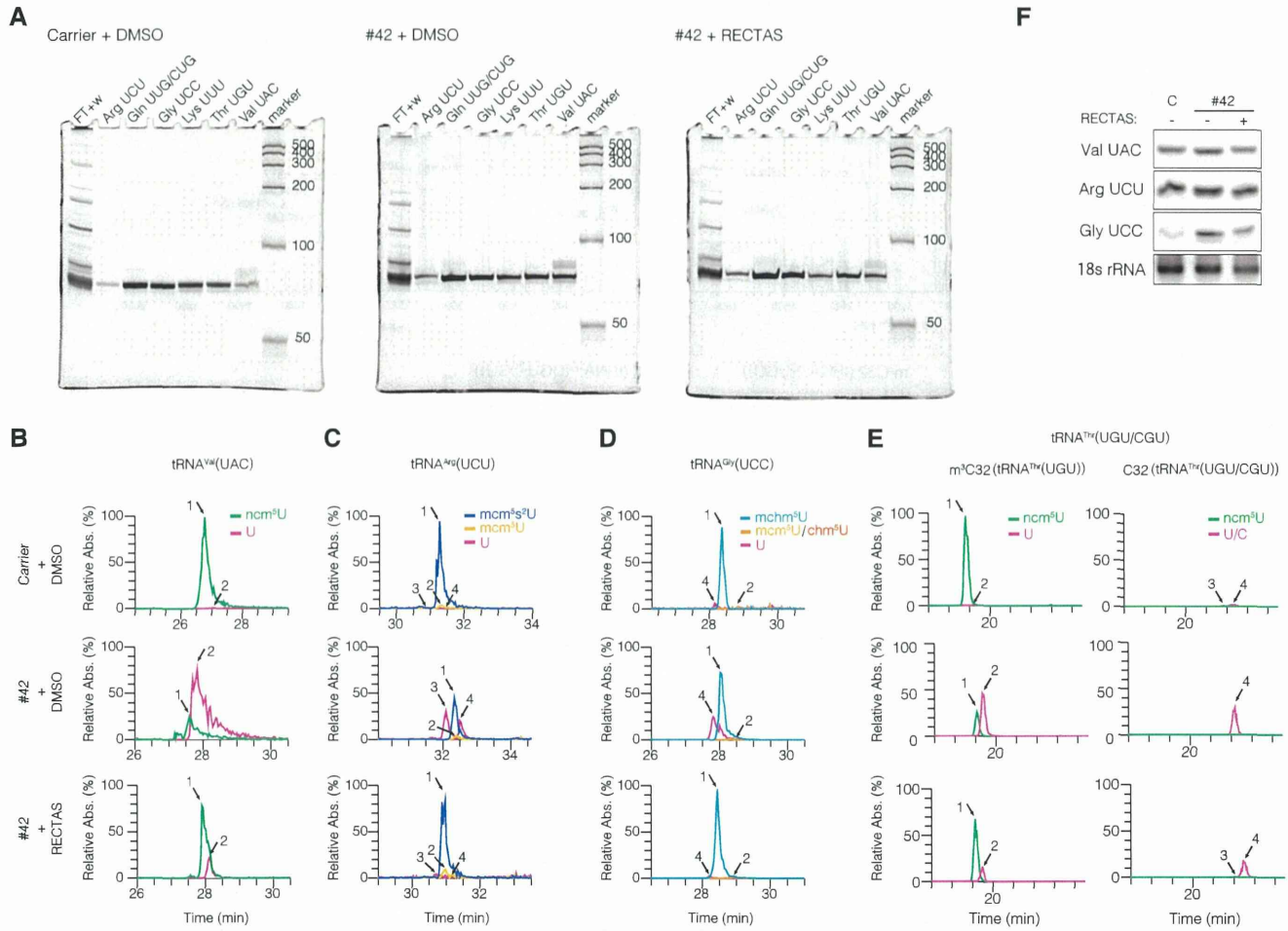

Fig. S6. Recovery of uridine modification of tRNAs by RECTAS in cells of patients with FD. (*A*) PAGE (10%, 7 M urea) of tRNAs from DMSO- or RECTAS-treated cells derived from patients with FD or a carrier, isolated by RCC. RNAs were visualized by SYBR Gold staining. (*B–E*) LC/MS analyses of the RNase T_1 fragments of tRNAs obtained from DMSO-treated Carrier cells (*Top*) and FD patient #42 cells treated with either 0.02% DMSO (*Middle*) or 2 μM RECTAS (*Bottom*). The mass chromatograms detecting RNase T_1 fragments harboring an unmodified or modified uridine residue for tRNA^{Val}(UAC) (*B*), tRNA^{Arg}(UCU) (*C*), tRNA^{Gly}(UCC) (*D*), and tRNA^{Thr}(UGU) (*E*) are shown as in Fig. 5 *B–D* and Fig. S5*E*. (*F*) Northern blot analysis of tRNAs Val(UAC), Arg(UCU), and Gly(UCC) in carrier (C) and FP patient #42 cells treated with DMSO or RECTAS. 18s rRNA was used as the loading control.

Table S1. Oligonucleotide sequences used in this study for plasmid construction, semiquantitative PCR, and the probes for RCC and Northern blotting

For the cloning of a genomic *IKBKAP* gene fragment of exon 19–21
- FW: 5′-ATACAAAAGTTGTTACAGGCCGGCCTGAGCAGCAAT-3′
- RV: 5′-GAAAGCTGGGTATGCATTCAAATGCCTCTTTAAACA-3′

For the introduction of FD mutation
- FW: 5′-TGGTTGGACAAGTAAGCGCCATTGTACTGTTTG-3′
- RV: 5′-CAAACAGTACAATGGCGCTTACTTGTCCAACCA-3′

For the introduction of single base deletion in exon 20 to adjust ORFs
- FW: 5′-GGTTTTAGCTCAGATCGGAAGTGGTTGGAC-3′
- RV: 5′-GTCCAACCACTTCCGATCTGAGCTAAAACC-3′

For semiquantitative PCR
- For endogenous *IKBKAP*
  - FW: 5′-GGATTGTCACTGTTGTGC-3′
  - RV: 5′-CAAGTTAATATGATTCACAGAATCT-3′
- For SPREADD reporters
  - FW: 5′-AGCATGGCCTTTGCAGGGCTGGC-3′
  - RV: 5′-TGACGTCCTCGGAGGAGGCGA-3′
- For endogenous *GAPDH*
  - FW: 5′-CCATCACCATCTTCCAGGAGCGAG-3′
  - RV: 5′-GTGATGGCATGGACTGTGGTCATG-3′

For amplification of the first part of *IKBKAP* Ex20-21WT/FD construction
- FW: 5′-GGGAAGCTTTCATCATCGAGCCCTGGTTTTAG-3′ (HindIII site italicized)
- RV: 5′-TTAGGTACCCGAAATTGTAATAAAATACTTATTG-3′ (KpnI site italicized)

For amplification of the second part of *IKBKAP* Ex20-21WT/FD construction
- FW: 5′-GTGGTACCTGATTTTTTTATTCTGTAATTTC-3′ (KpnI site italicized)
- RV: 5′-GATGGATCCGGGGACCACTTTGTAC-3′ (BamHI site italicized)

For construction of *IKBKAP* int-Ex20-int WT and *IKBKAP* int-Ex20-int FD
- FW: 5′-AACAAGCTTCTGCTAAAAGTGTGCTG-3′ (HindIII site italicized)
- RV: 5′-TTAGGTACCCGAAATTGTAATAAAATACTTATTG-3′ (KpnI site italicized)

For each tRNA purification by RCC and Northern blot probe
- $tRNA^{Val}$(UAC): 5′-TGGTTCCACTGGGGCTCGAACCCAGGACCTTCTGC-3′
- $tRNA^{Arg}$(UCU): 5′-GAAGTCCAATGCGCTATCCATTGCGCCACAGAGCC-3′
- $tRNA^{Gly}$(UCC): 5′-GAAGGCAGCTATGCTCACCACTATACCACCAACGC-3′
- $tRNA^{Thr}$(UGU): 5′-GGCTCCATAGCTCAGGGGTTAGAGCACTGGTCTTG-3′

FW, forward, RV, reverse.

Table S2. List of RNase T_1 fragments detected in the mass chromatograms shown in Figs. 5 and 6 and Figs. S5 and S6

tRNA	Sequence of T_1 fragments	*m/z*	Charge state	Depicted color	Peak no.
$tRNA^{val}$ (UAC)	CUUncm^{5}UACACGp	726.833	(−4)	Green	1
	CUUUACACGp	712.583	(−4)	Magenta	2
$tRNA^{Arg}$ (UCU)	Am^{3}CUmcm^{5}s^{2}UCUt^{6}AAUUCAACGp	717.517	(−7)	Blue	1
	Am^{3}CUmcm^{5}UCUt^{6}AAUUCAACGp	715.235	(−7)	Yellow	2
	Am^{3}CUUCUt^{6}AAUUCAACGp	704.946	(−7)	Magenta	3
	ACUUCUt^{6}AAUUCAACGp	702.944	(−7)	Magenta	4
$tRNA^{Gly}$ (UCC)	CCUmchm^{5}UCCAAGp	734.341	(−4)	Light blue	1
	CCUmchm^{5}UCCAAGp + CCUmcm^{5}UCCAAG*	730.837, 730.342	(−4)	Orange	2
	CCmUUCCAAGp	715.841	(−4)	Magenta	3
	CCUUCCAAGp	712.337	(−4)	Magenta	4
$tRNA^{Thr}$ (UGU)	Um^{3}CUncm^{5}UGp	827.598	(−2)	Green	1
	Um^{3}CUUGp	799.088	(−2)	Magenta	2
	UCUncm^{5}UGp	820.591	(−2)	Green	1
	UCUUGp + UCUCGp*	792.08, 791.588	(−2)	Magenta	2

The nucleotide sequences of RNase T_1 fragments from each tRNA are shown with the *m/z*, charge state, and depicted color in Figs. 5 and 6. The wobble uridines are described in bold letters.

*Fragments marked could not been separated due to the adjacent *m/z* in LC/MS-MS.

ます．また，*EPH1* 遺伝子がかかわる老化制御経路を標的とした阻害剤を開発し，切り花の日持ちを延ばす技術につなげたいと考えています．

7月9日 朝日新聞

より多様なウイルスに効く次世代抗ウイルス薬を開発

萩原正敏（はぎわらまさとし）教授（京都大学大学院医学研究科）に聞く

Q この研究に取り組んだ経緯を教えてください．

従来の抗ウイルス薬はウイルスのタンパク質を薬効標的としているため，薬が効かない「耐性」を獲得したウイルスの出現が臨床現場で問題となっています．そこで私たちは，ウイルスが宿主細胞のタンパク質をうまく利用して自己複製している点に注目し，RNA転写を制御している宿主タンパク質“CDK9”を標的とした次世代抗ウイルス薬「FIT-039」の開発を行いました．

Q この化合物（次世代抗ウイルス薬）の特徴は何ですか？

FIT-039はCDK9を阻害することによりウイルスのRNA転写を抑制し抗ウイルス効果を発揮します．このとき，宿主のRNA転写はCDK9と同様の機能をもつ別のタンパク質が代替できるため，細胞増殖などには影響がないことを確認しています．多くのウイルスが自己複製にCDK9を必要としていますので，FIT-039はヘルペスウイルス，アデノウイルス，インフルエンザウイルスなどいろいろなウイルスに対する薬効を示しました．さらに，従来の抗ウイルス薬「アシクロビル」が効かないアシクロビル耐性ヘルペスウイルスを感染させたマウスに対しても，FIT-039は治療効果を示しました（図1）．

Q この成果をもとにどのような研究を進めていくのでしょうか．

FIT-039は次世代抗ウイルス薬として臨床現場および国内外の製薬会社からも注目を集めています．そして現在，ヒトパピローマウイルス性疾患をはじめとするさまざまなウイルス性疾患に対する治療効果に関する研究を行っています．

また，基礎研究と並行して医師主導型臨床治験の準備も進めており，一刻も早い実用化を目指しています．

図1　従来薬耐性ヘルペスウイルス皮膚感染マウスモデルにおける治療効果

も役立つという．（7/8日本経済新聞）

●レアメタルを使わない充電池

安価なマグネシウムを使って，リチウムイオン充電池の1/10以下の材料費で同等以上に電気を蓄える充電池が開発された．内本喜晴教授（京都大学）らは，負極に純粋なマグネシウム，正極にマグネシウムと鉄などの化合物を使い，電極間を満たす電解液もマグネシウムを含む溶液にすることで，電極に被膜が形成しないようにした．将来，高価なレアメタルを使わない充電池が実現するかもしれない．（7/12読売新聞）

●安価な触媒でつくる導電性高分子

三治敬信特任教授（東京工業大学）らは，有機ELや有機太陽電池の材料となる導電性高分子を従来よりも安価な触媒で合成する技術を開発した．これまでの触媒は高価な貴金属などを含み，約100℃で数時間の熱処理が必要なうえ分子量も不揃いであったが，有機材料を改良した新たな触媒により，室温で大きさがほぼ揃った高分子を数分間で合成できる．（7/15日本経済新聞）

●匂いと食欲のつながりが明らかに！

食べ物の匂いにハエが集まる理由を尾崎まみこ教授（神戸大学）らが突き止めた．クロキンバエを使って嗅覚と味覚の神経の伝達方法を調べたところ，ハエの口のすぐ上にある副嗅覚器から延びる神経の一端が分岐し，それが味覚の情報が集まる脳の部位に到達していることがわかった．また，砂糖水にハエが好む匂いをつけると，匂いがない場合に比べて食欲が3割増すが，副嗅覚器を切断するとその反応がなくなることも明らかにされた．（7/17毎日新聞）

●心臓の冠静脈をつくるしくみを解明

心臓の表面を走る冠静脈がつくられるしくみが解明された．中岡良和助教（大阪大学）らはマウスの胎児を使った実験で，心筋細胞が分泌するアンジオポエチン1（Ang1）というタンパク質が，ほかの細胞に働きかけて冠静脈をつくっていたことを突き止めた．心筋梗塞などで詰まった血管を，新しい血管で代替する治療の開発につながる成果だという．（7/23京都新聞）

RNA 病

RNA disease

京都大学大学院医学研究科
形態形成機構学
木村　亮（KIMURA Ryo）
萩原正敏（HAGIWARA Masatoshi）

はじめに

近年，遺伝子発現制御機構の解明が進み，RNA が多様な機能を有することが明らかになってきた．RNA は転写後，切断・修飾などを受ける．前駆体 mRNA プロセシングという過程を経て成熟 mRNA となる．この過程は，遺伝情報の発現に必須であるとともに，遺伝子発現を精巧に調節することができ，RNA 結合蛋白質や non-coding RNA もかかわっている．RNA プロセシング異常は，さまざまな疾患を引き起こすことから，RNA プロセシング異常に起因する疾患群を総称して，「RNA 病（RNA disease）」という[1]．

遺伝子発現の各ステップ

DNA から転写された前駆体 mRNA には，5' 末端に 7-メチルグアノシンからなるキャップ構造が付加される．その後，3' 末端にアデニンが 200 個以上からなるポリ A 鎖が付加される．キャップ構造やポリ A 鎖は，mRNA の安定性などに関与する．

さらにスプライシングとよばれる，イントロンを除去し，エクソン同士をつなぐ反応の後，成熟 mRNA は，エクソン接合部複合体（exon junction complex：EJC）などの働きで核から細胞質へ輸送後，蛋白質へと翻訳される．一方，異常な mRNA は，NMD（nonsense-mediated mRNA decay）などの mRNA 監視機構を通じて，選択的に分解される（**図 1**）．RNA 結合蛋白質や non-coding RNA を含む上記プロセスの異常により，RNA 病が生じる[2]．

RNA スプライシング異常に起因する疾患

真核生物では 1 種類の前駆体 mRNA から異なるパターンのエクソン選択により，複数種の mRNA が産生される場合が多数ある．この過程は選択的スプライシングとよばれており，遺伝子発現の多様性を担っている．近年，スプライシング機構の破綻がさまざまな疾患を引き起こすことが明らかになってきている．

神経疾患領域では，脊髄性筋萎縮症（spinal muscular atrophy：SMA），筋ジストロフィー，家族性前頭側頭型認知症（frontotemporal dementia and parkinsonism linked to chromosome 17：FTDP-17），脆弱 X 症候群，Prader-Willi 症候群（Prader-Willi syndrome：PWS），Rett 症候群，脊髄小脳失調症 8 型（spinocerebellar ataxia type 8：SCA8），筋萎縮性側索硬化症（amyotrophic lateral sclerosis：ALS），家族性自律神経失調症などがある．一方，精神疾患領域では，統合失調症，自閉症との関連が報告されている．

エクソンスキッピング法による治療

デュシェンヌ型筋ジストロフィー（Duchenne muscular dystrophy：DMD）は，伴性劣性遺伝形式をとる最も頻度の高い遺伝性進行性筋萎縮症である．X 染色体短腕にあるジストロフィン遺伝子のエクソン欠失変異により，筋肉のジストロフィン蛋白が欠損．その結果，3 歳ごろから進行性の筋力低下が出現し，20 歳代には呼吸不全などで死に至る疾患である．

ジストロフィン遺伝子は，79 のエクソンから構成される非常に大きな遺伝子であり，くり返し構造を有することから，一部を欠失しても機能を保つことができる．そのため，特定のエクソンを取り除き，短い mRNA が合成されても，正常のジストロフィン蛋白より短くなるが，ほぼ正常な機能をもつジストロフィンが合成される[3]．現在，エクソンスキップを誘導するアンチセンス核酸や低分子化合物の探索・開発が進められており[4]，わが国においてもこれらを用いた臨床試験が開始されている（**図 2**）．

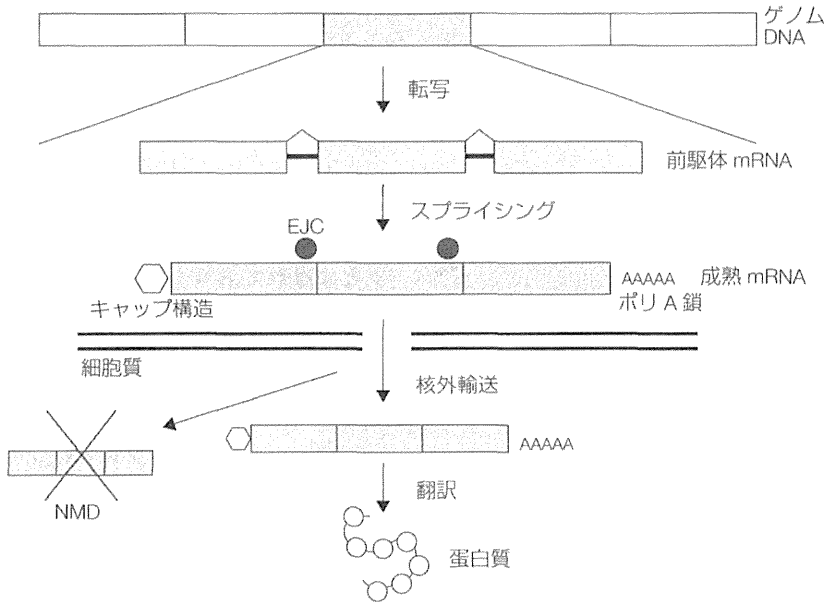

図 1. 遺伝子発現の各ステップ

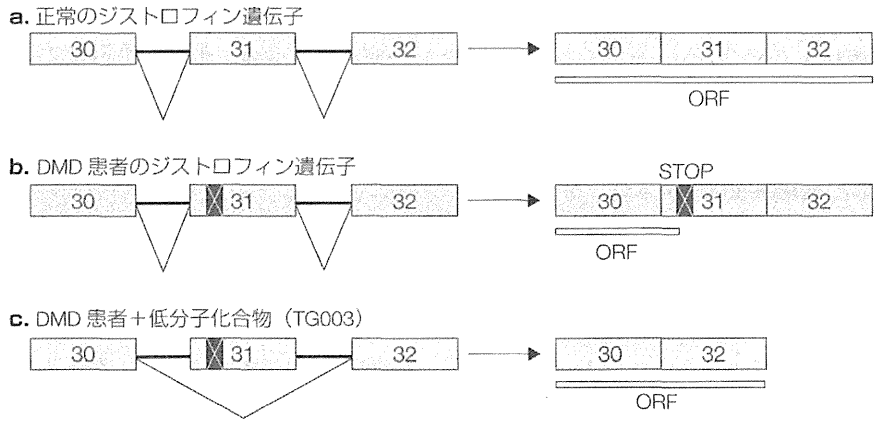

図 2. 低分子化合物を用いた DMD に対するエクソンスキッピング法

おわりに

RNA 病は，RNA プロセシング異常によって生じる病態の総称である．エクソンスキッピング法は，RNA 病治療の可能性を示唆しており，今後，さまざまな遺伝性疾患や神経・精神疾患への応用が期待されている．

文　献

1) 片岡直行：RNA スプライシング異常と疾患．遺伝子医学 MOOK4，174-180，2006
2) 萩原正敏：RNA プロセシング異常．細胞工学 **29**：126-130，2010
3) 稲田利文：生命分子を統合する RNA のもつ多様な情報と機能．実験医学 **31**：1086-1092，2013
4) Nishida A, Kataoka N, Takeshima Y *et al*：Chemical treatment enhances skipping of a mutated exon in the dystrophin gene. *Nat Commun* **2**：308, 2011